


1716
NACA TN 2784

TECH LIBRARY KAFB, NM
0065925


NATIONAL ADVISORY COMMITTEE FOR AERONAUTICS

TECHNICAL NOTE 2784

METHOD FOR CALCULATION OF COMPRESSIBLE LAMINAR
BOUNDARY-LAYER CHARACTERISTICS IN AXIAL
PRESSURE GRADIENT WITH ZERO
HEAT TRANSFER

By Morris Morduchow and Joseph H. Clarke
Polytechnic Institute of Brooklyn



Washington
September 1952

AFM. C
TECHNICAL LIBRARY
AFL 2811



NATIONAL ADVISORY COMMITTEE FOR AERONAUTICS

TECHNICAL NOTE 2784

METHOD FOR CALCULATION OF COMPRESSIBLE LAMINAR
BOUNDARY-LAYER CHARACTERISTICS IN AXIAL
PRESSURE GRADIENT WITH ZERO
HEAT TRANSFER

By Morris Morduchow and Joseph H. Clarke

SUMMARY

The Kármán-Pohlhausen method is extended primarily to sixth-degree velocity profiles for determining the characteristics of the compressible laminar boundary layer over an adiabatic wall in the presence of an axial pressure gradient. It is assumed that the Prandtl number is unity and that the coefficient of viscosity varies linearly with the temperature. A general approximate solution which permits a rapid determination of the boundary-layer characteristics for any given free-stream Mach number and given velocity distribution at the outer edge of the boundary layer is obtained. Numerical examples indicate that this solution will in practice lead to results of satisfactory accuracy, including the critical Reynolds number for stability. For the special purpose of calculating the location of the separation point in an adverse pressure gradient, a short and simple method, based on the use of a seventh-degree velocity profile, is derived. The numerical example given here indicates that this method should in practice lead to sufficiently accurate results. For the special case of flow near a forward stagnation point it is shown that the Kármán-Pohlhausen method with the usual fourth-degree profiles leads to results of adequate accuracy, even for the critical Reynolds number.

INTRODUCTION

In reference 1 it was concluded that from the viewpoint of both accuracy and convenience of calculation a suitable method for determining the characteristics of a compressible laminar boundary layer is that based on an extension of the Kármán-Pohlhausen integral method to velocity profiles of higher degree than the fourth, especially sixth degree. An ordinary differential equation for general types of flow was derived, but only the flow over a flat plate at zero incidence was

investigated in detail. The purpose of the present investigation is to apply explicitly this method to flows with axial pressure gradients.

The ordinary differential equation derived in reference 1 is converted here into a convenient nondimensional form, and a general approximate solution of this equation in closed form is then derived. By means of this solution the physically significant boundary-layer characteristics of the flow over an insulated wall can be calculated fairly easily and quickly for any given free-stream Mach number and for any given velocity distribution outside of the boundary layer. For particular accuracy in determination of the separation point in an adverse pressure gradient, a simple method based on the use of a seventh-degree velocity profile, which, in accordance with a suggestion of Timman (reference 2), is made to satisfy an additional condition at the separation point, is derived.

For illustrative purposes, two simple but basically different types of flow are treated in detail. In the first example flow with a linearly diminishing velocity at the outer edge of the boundary layer is considered. Such a flow is of particular interest here because it represents the simplest case of an adverse pressure gradient and because the usual application of the Kármán-Pohlhausen method with fourth-degree velocity profiles has been known to lead to highly inaccurate results in such cases (cf., e.g., reference 3). The skin friction, velocity profiles, and critical Reynolds number are calculated for several Mach numbers in this case by means of the general solution derived here. These results are then compared with known series solutions of the partial differential equations (references 4 and 5) for this case; the agreement is shown to be satisfactory for practical purposes. This agreement includes critical Reynolds numbers for laminar-flow stability and location of the separation point. In connection with the latter it is significant to note that for zero Mach number the Kármán-Pohlhausen method with fourth-degree velocity profiles leads to an error of about 30 percent in predicting the separation point, while the use of a sixth-degree profile reduces this error to 15 percent, and the special use of a seventh-degree profile for this (and only this) purpose practically eliminates the error for all Mach numbers (0 to 3) considered numerically here.

The second example treated is the flow near a forward stagnation point. This case is of interest not only because it may represent the subsonic flow over a blunt nose but also because it had already been found by Schlichting and Ulrich (reference 6) that in such a case no physically significant values can be found for the boundary-layer thickness when sixth-degree profiles are used. It is shown in the present investigation that although this is, strictly speaking, true, an approximate value for the thickness is nevertheless obtainable. It is also shown that in this case the usual type of application of the Kármán-Pohlhausen method with fourth-degree velocity profiles leads not only

to real values of the boundary-layer thickness but also to results of satisfactory accuracy, even for the critical Reynolds number. Consequently, in such a case fourth-degree profiles may be used with confidence in the accuracy of the results to be obtained.

As in reference 1, it has been assumed that the viscosity coefficient is directly proportional to the absolute temperature, and that, following a suggestion of Chapman (references 7 and 8), the constant of proportionality may be chosen so that Sutherland's relation is exactly satisfied at the wall. This introduces considerable mathematical simplification and will lead in practice to fairly accurate results at least for lower Mach numbers (below 5). For the same reasons it has also been assumed that the Prandtl number is unity, and this may be viewed as an approximation for air, where the Prandtl number is more nearly 0.72.

This work, carried out at the Polytechnic Institute of Brooklyn Aeronautical Laboratories, was sponsored by and conducted with the financial assistance of the National Advisory Committee for Aeronautics.

SYMBOLS

| | |
|--------------------------|---|
| a_2 | coefficient of τ^2 in velocity profile; also given by equation (20) |
| \bar{a}_2 | constant "average" value of a_2 |
| b | constant in given velocity distribution $u_1/u_\infty(\xi)$, equations (27a) and (30a) |
| C | factor of proportionality in equation $\mu/\mu_\infty = C(T/T_\infty)$ |
| C_f | skin-friction coefficient $\left((\mu \partial u / \partial y)_0 / (\rho_\infty u_\infty^2 / 2) \right)$ |
| c_p, c_v | specific heats at constant pressure and at constant volume, respectively |
| F_1, F_2, F_3 | integrals defined by equations (12) |
| F_{1s}, F_{2s}, F_{3s} | values of F_1 , F_2 , and F_3 based on seventh-degree profiles; given by equations (B2) |

| | |
|------------------|---|
| G | constant defining strength of a shock wave in flow outside of boundary layer; given by equation (19e) |
| I | integrating factor of equation (21) |
| K | constant defined by equations (18a) and (18b) |
| k | thermal conductivity of fluid |
| L | characteristic length; see equations (13) |
| l | characteristic length in stability calculations (appendix C) |
| M | Mach number |
| p | pressure |
| R | Reynolds number |
| R_∞ | free-stream Reynolds number $(\rho_\infty u_\infty L / \mu_\infty)$ |
| S | Sutherland's constant, defined by equation (8); for air, $S = 216^\circ \text{R}$ |
| T | absolute temperature |
| t | transformation variable defined by equation (10) |
| u, v | velocity components in x- and y-directions, respectively |
| x, y | coordinates parallel and perpendicular to surface, respectively |
| α, β | quantities defined by equations (C2) |
| γ | ratio of specific heats (c_p/c_v) ; for air, $\gamma = 1.4$ |
| δ | physical boundary-layer thickness in xy-plane |
| δ_t | boundary-layer thickness in xt-plane |
| $\eta = 1 - \xi$ | |

$$\lambda = \frac{1}{C} R_\infty \left(\frac{\delta_t}{L} \right)^2$$

| | |
|-------------|--|
| λ_s | value of λ based on seventh-degree profiles and used only for determining separation point |
| μ | coefficient of viscosity |
| ν | kinematic viscosity (μ/ρ) |
| ξ | dimensionless distance along wall (x/L) |
| ρ | mass density |
| τ | dimensionless variable (t/δ_t) |

Subscripts

| | |
|----------|--|
| o | values at wall, for example, T_o |
| l | local values at outer edge of boundary layer; for example, M_l , T_l , and u_l |
| a | initial value in region of adverse pressure gradient (appendix B) |
| b | values immediately behind a shock wave at leading edge |
| c | values at critical point for stability (appendix C) |
| s | value based on seventh-degree profiles |
| ∞ | values in undisturbed free stream; for example, M_∞ , T_∞ , and u_∞ |

A prime (') denotes at first differentiation with respect to x . In equation (14) and thereafter in the main text, a prime denotes differentiation with respect to ξ . In appendix C, it denotes differentiation with respect to y/l .

BASIC EQUATIONS

Two-Dimensional Compressible Flow

The following equations characterize the steady two-dimensional compressible flow of a gas in the laminar boundary layer over a surface of large radius of curvature compared with the boundary-layer thickness:

$$\rho u \frac{\partial u}{\partial x} + \rho v \frac{\partial u}{\partial y} = \rho_1 u_1 u_1' + \frac{\partial}{\partial y} \left(\mu \frac{\partial u}{\partial y} \right) \quad (1)$$

$$\rho u c_p \frac{\partial T}{\partial x} + \rho v c_p \frac{\partial T}{\partial y} = -\rho_1 u_1 u_1' u + \frac{\partial}{\partial y} \left(k \frac{\partial T}{\partial y} \right) + \mu \left(\frac{\partial u}{\partial y} \right)^2 \quad (2)$$

$$\frac{\partial}{\partial x}(\rho u) + \frac{\partial}{\partial y}(\rho v) = 0 \quad (3)$$

$$\frac{\rho}{\rho_1} = \frac{T_1}{T} \quad (4)$$

Equations (1) and (2) are the momentum and energy equations, respectively. The equation of continuity is given by expression (3), while equation (4) follows from the ideal gas law. In equations (1), (2), and (4) account has been taken of the well-known implication of Prandtl's basic boundary-layer assumption that the pressure gradient $\partial p/\partial y$ across the boundary-layer thickness is zero. Thus the axial pressure gradient can be considered as given by the Bernoulli equation

$$\frac{\partial p}{\partial x} = -\rho_1 u_1 u_1' \quad (5)$$

where the subscript 1 refers to the potential flow over the surface streamline outside of the boundary layer. This potential flow is assumed to be known.

For a Prandtl number $\mu c_p/k$ of unity and zero heat transfer at the wall ($\partial T/\partial y = 0$ at $y = 0$) it can be shown, by eliminating $\rho_1 u_1 u_1'$ from equations (1) and (2), that

$$\frac{u^2}{2} + c_p T = \text{Constant} \quad (6)$$

Equation (6) can be expressed in the following nondimensional form:

$$\frac{T}{T_1} = 1 + \frac{\gamma - 1}{2} M_1^2 \left(1 - \frac{u^2}{u_1^2} \right) \quad (6a)$$

Thus the energy equation (2) can for this case be replaced by equation (6a), which gives the temperature explicitly as a simple function of the velocity. This case of unit Prandtl number and zero heat transfer is the one which will be treated in the present analysis.

It will be assumed here, as in references 1, 7, and 8, that the viscosity coefficient can be expressed as a linear function of the temperature in the form

$$\frac{\mu}{\mu_{\infty}} = C \frac{T}{T_{\infty}} \quad (7)$$

where C is a constant determined so that relation (7) will give the same value of μ at the wall as the Sutherland viscosity-temperature relation. The latter relation is generally assumed to be accurate at least below the hypersonic range. Thus

$$C = \left(\frac{T_0}{T_{\infty}}\right)^{1/2} \frac{1 + (S/T_{\infty})}{(T_0/T_{\infty}) + (S/T_{\infty})} \quad (8)$$

where S is a constant which for air has the value $S = 216^{\circ} \text{R}$. From equation (6a) it follows that the wall temperature T_0 as a function of the free-stream Mach number M_{∞} will be:

$$\frac{T_0}{T_{\infty}} = 1 + \left(\frac{\gamma - 1}{2}\right) M_{\infty}^2 \quad (9)$$

Hence the constant C will be a function of the Mach number M_{∞} and the free-stream temperature T_{∞} .

By integrating equation (1) with respect to y across the boundary-layer thickness $y = 0$ to $y = \delta$ and introducing the Dorodnitzyn variable t defined by the transformation

$$y = \int_0^t \frac{T}{T_1} dt \quad (10)$$

the following equation, essentially the Kármán integral momentum equation for compressible laminar boundary layers, can be derived (cf. reference 1, equation (24)):

$$\frac{1}{2} F_1 (\delta_t^2)' + \left[F_1' + F_1 (\log_e \rho_1 u_1^2)' - F_2 (\log_e u_1)' \right] \delta_t^2 = F_3 \frac{\mu_\infty C}{\rho_1 u_1} \frac{T_1}{T_\infty} \quad (11)$$

Here

$$\left. \begin{aligned} F_1 &= \int_0^1 \frac{u}{u_1} \left(1 - \frac{u}{u_1} \right) d\tau \\ F_2 &= \int_0^1 \left(\frac{u}{u_1} - \frac{T}{T_1} \right) d\tau \\ F_3 &= \left[\frac{\partial}{\partial \tau} \left(\frac{u}{u_1} \right) \right]_0 \end{aligned} \right\} \quad (12)$$

and δ_t , the value of t when $y = \delta$, is the boundary-layer thickness in the xt -plane, while $\tau = t/\delta_t$.

Introducing the dimensionless variables λ and ξ defined by

$$\left. \begin{aligned} \lambda &= \frac{1}{C} R_\infty \left(\frac{\delta_t}{L} \right)^2 \\ \xi &= \frac{x}{L} \end{aligned} \right\} \quad (13)$$

where L is a characteristic length and $R_\infty = \rho_\infty u_\infty L / \mu_\infty$ is the free-stream Reynolds number, equation (11) can be written as

$$\lambda' + 2\lambda \left[\frac{\rho_1'}{\rho_1} + \frac{F_1'}{F_1} + \frac{u_1'}{u_1} \left(2 - \frac{F_2}{F_1} \right) \right] = 2 \frac{u_\infty}{u_1} \frac{\rho_\infty}{\rho_1} \frac{T_1}{T_\infty} \frac{F_3}{F_1} \quad (14)$$

where the primes henceforth denote differentiation with respect to ξ .

Velocity Profiles

If a definite form of profile for u/u_1 as a function of τ is assumed, then equation (14) becomes an ordinary differential equation in $\lambda(\xi)$. In the present analysis, sixth-degree profiles will be assumed for most cases and will be chosen to satisfy appropriate boundary conditions at the wall and at the outer edge of the boundary layer. This is in accordance with the results of reference 1, where it was concluded that, with the possible exceptions of determination of separation point in an adverse pressure gradient and of calculation of the boundary layer in the vicinity of a stagnation point, the use of sixth-degree profiles should for practical purposes lead to sufficiently accurate determination of laminar-boundary-layer characteristics, including critical Reynolds number for stability. Sixth-degree profiles have also been applied recently by Weil (reference 9).

The following boundary conditions, expressed in the xt -plane, will be satisfied:

At $\tau = 0$:

$$\left. \begin{aligned} \frac{u}{u_1} &= 0 \\ \frac{\partial^2(u/u_1)}{\partial \tau^2} &= -\left(\frac{T_\infty}{T_1}\right)^2 \frac{\rho_1(u_1)}{\rho_\infty(u_\infty)} \frac{T_0}{T_\infty} \lambda \\ \frac{\partial^3(u/u_1)}{\partial \tau^3} &= 0 \end{aligned} \right\} \quad (15)$$

At $\tau = 1$:

$$\left. \begin{aligned} \frac{u}{u_1} &= 1 \\ \frac{\partial(u/u_1)}{\partial \tau} = \frac{\partial^2(u/u_1)}{\partial \tau^2} = \frac{\partial^3(u/u_1)}{\partial \tau^3} &= 0 \end{aligned} \right\}$$

It should be noted that the second condition at the wall ($\tau = 0$) in equations (15) follows in general from the original partial differential equation (1) in conjunction with equation (7). The third condition at the wall follows from differentiation of equation (1) with respect to t , in conjunction with the condition of zero heat transfer $((\partial T / \partial \tau)_0 = 0)$ at the wall. The second and third conditions of equations (15), moreover, are valid only for zero normal velocity at the wall.

The sixth-degree polynomial satisfying conditions (15) is found to be

$$\frac{u}{u_1} = 2\left(1 - \frac{a_2}{5}\right)\tau + a_2\tau^2 - (5 + 2a_2)\tau^4 + 2(3 + a_2)\tau^5 - \left(2 + \frac{3}{5}a_2\right)\tau^6 \quad (16)$$

where:

$$a_2 = -\frac{\lambda}{2} \frac{u_1'}{u_\infty} \frac{T_0}{T_\infty} \frac{\rho_1}{\rho_\infty} \left(\frac{T_\infty}{T_1}\right)^2 \quad (17)$$

Substitution of equation (16) into equations (12) leads to the following explicit expressions for F_1 , F_2 , and F_3 in terms of a_2 :

$$\left. \begin{aligned} F_1 &= 0.1093 + 0.00211a_2 - 0.000622a_2^2 \\ F_2 &= -0.2857 - 0.01905a_2 - \frac{\gamma - 1}{2} M_1^2 (0.3950 + \\ &\quad 0.02116a_2 - 0.000622a_2^2) \\ F_3 &= 2 - 0.4000a_2 \end{aligned} \right\} \quad (18)$$

By substituting expressions (18) and (17) into equation (14), the latter becomes an ordinary differential equation of the first order in $\lambda(\xi)$.

The quantities with subscript 1 may be regarded as given functions of ξ from the potential flow outside of the boundary layer. From the relation $(u^2/2) + c_p T = \text{Constant}$, which is valid outside of the boundary layer even across a shock wave, it follows that

$$\frac{T_1}{T_\infty} = 1 + \left(\frac{\gamma - 1}{2}\right) M_\infty^2 \left(1 - \frac{u_1^2}{u_\infty^2}\right) \quad (19a)$$

Moreover, the local Mach number M_1 can be expressed by:

$$M_1^2 = M_\infty^2 \left(\frac{u_1}{u_\infty} \right)^2 \left(\frac{T_1}{T_\infty} \right)^{-1} \quad (19b)$$

If there are no shock waves, the flow outside of the boundary layer may be considered as isentropic, so that the relation

$$\frac{\rho_1}{\rho_\infty} = \left(\frac{T_1}{T_\infty} \right)^{1/(\gamma-1)} \quad (19c)$$

is valid. In the presence of a shock wave, the flow may be considered as isentropic before and behind, though not across, the wave. In that case, equation (19c) may be modified to

$$\frac{\rho_1}{\rho_\infty} = G \left(\frac{T_1}{T_\infty} \right)^{1/(\gamma-1)} \quad (19d)$$

where G is a constant given by

$$G = \left(\frac{\rho_b}{\rho_\infty} \right) \left(\frac{T_b}{T_\infty} \right)^{-1/(\gamma-1)} \quad (19e)$$

while ρ_b and T_b are the values of ρ and T immediately behind the wave, and ρ_1 and T_1 refer to the region behind the wave at the outer edge of the boundary layer. Relation (19c) can be considered as a special case of relation (19d), namely the case of $G = 1$. The ratios ρ_b/ρ_∞ and T_b/T_∞ may be considered as known from the given flow outside of the boundary layer.

By the use of equations (9), (19a), and (19d) the expression (17) for a_2 can be written, more explicitly, as

$$a_2 = -\frac{\lambda}{2} \frac{u_1'}{u_\infty} G \left(1 + \frac{\gamma-1}{2} M_\infty^2 \right) \left[1 + \left(\frac{\gamma-1}{2} M_\infty^2 \left(1 - \frac{u_1^2}{u_\infty^2} \right) \right)^{\frac{3-2\gamma}{\gamma-1}} \right] \quad (20)$$

GENERAL SOLUTIONS OF EQUATIONS

For a given potential-flow velocity distribution $u_1/u_\infty(\xi)$ and Mach number M_∞ , the differential equation (14) can be solved for $\lambda(\xi)$ without any basic difficulties by well-known numerical methods, such as Adam's method or the Runge-Kutta method (cf., e.g., reference 10). Such a straightforward procedure may in practice nevertheless be tedious. A relatively simple general approximate solution of equation (14) will therefore be derived in this section. This solution will be found to be sufficiently accurate for most practical purposes.

General Approximate Solution

The solution to be derived here will be based on the approximating assumption that in the expressions for F_1 and F_2 the quantities a_2 and a_2^2 as given by equation (20) may be replaced by constant "average" values \bar{a}_2 and $\overline{a_2^2}$ for the flow. This assumption is justified by the fact that in expressions (18) for F_1 and F_2 the a_2 terms are relatively small; hence even large errors in the evaluation of a_2 will lead to only small errors in the evaluation of F_1 and F_2 .

By replacing a_2 and a_2^2 by constant average values \bar{a}_2 and $\overline{a_2^2}$ in expressions (18) for F_1 and F_2 , the quantity F_1 becomes a constant, while F_2 can be written as

$$F_2 = -0.2857 - 0.01905\bar{a}_2 - \left(\frac{\gamma - 1}{2}\right)KM_1^2 \quad (18a)$$

where K is a constant given by

$$K = 0.3950 + 0.02116\bar{a}_2 - 0.000622\overline{a_2^2} \quad (18b)$$

By use of the relation

$$\frac{T_0}{T_1} = 1 + \left(\frac{\gamma - 1}{2}\right) M_1^2$$

which follows from equation (6a), and by insertion of expression (18a) for F_2 , expression (18) for F_3 , and expression (17) for a_2 in the right side of equation (14), the latter equation can be written in the form:

$$\lambda' + 2\lambda \left\{ \frac{\rho_1'}{\rho_1} + \frac{u_1'}{u_1} \left[2 + \frac{1}{F_1} (0.08571 + 0.01905\bar{a}_2) + \left(\frac{\gamma - 1}{2}\right) \left(K - \frac{1}{5}\right) \frac{1}{F_1} M_1^2 \right] \right\} = \frac{4}{F_1} \frac{u_\infty}{u_1} \frac{\rho_\infty}{\rho_1} \frac{T_1}{T_\infty} \quad (21)$$

Equation (21) is now a linear differential equation of the first order in λ . By use of relations (19a), (19b), and (19d) it will be found that an integrating factor I of equation (21) is:

$$I = \left(\frac{u_1}{u_\infty}\right)^{4 + \frac{2}{F_1} (0.08571 + 0.01905\bar{a}_2)} \left(\frac{T_1}{T_\infty}\right)^{\frac{2}{\gamma-1} - \frac{1}{F_1} \left(K - \frac{1}{5}\right)}$$

The solution of equation (21) satisfying the boundary condition $\lambda = 0$ or some finite value (in the case of a stagnation point at $\xi = 0$) at $\xi = 0$ is then:

$$\lambda = \frac{4}{F_1 G} \frac{\int_0^\xi \left(\frac{u_1}{u_\infty}\right)^{3 + \frac{2}{F_1} (0.08571 + 0.01905\bar{a}_2)} \left(\frac{T_1}{T_\infty}\right)^{\frac{\gamma}{\gamma-1} - \frac{1}{F_1} (0.1950 + 0.02116\bar{a}_2 - 0.000622\bar{a}_2^2)} d\xi}{\left(\frac{u_1}{u_\infty}\right)^{4 + \frac{2}{F_1} (0.08571 + 0.01905\bar{a}_2)} \left(\frac{T_1}{T_\infty}\right)^{\frac{2}{\gamma-1} - \frac{1}{F_1} (0.1950 + 0.02116\bar{a}_2 - 0.000622\bar{a}_2^2)}} \quad (22)$$

where T_1/T_∞ is obtained from equation (19a).

For a given velocity distribution $u_1/u_\infty(\xi)$, the effect of Mach number M_∞ is given by the T_1/T_∞ terms in equation (22) and, in the case of a shock wave at the leading edge, also by the constant G (cf. equation (19e)). If the flow over a given object is considered, however, then the Mach number effect will be contained also in the u_1/u_∞ terms, since the velocity distribution u_1/u_∞ will then be a function of Mach number.

The integral in equation (22) can in practice be evaluated without difficulty by numerical means such as Simpson's rule (cf., for example, reference 10). An average value \bar{a}_2 for a_2 can, in any given case, be chosen by considering equation (20).

Boundary-Layer Characteristics

Once $\lambda(\xi)$ has been determined, the boundary-layer characteristics follow from the equations developed here. Thus the local skin-friction coefficient C_f will be:¹

$$C_f = \frac{(\mu \partial u / \partial y)_o}{\rho_\infty u_\infty^2 / 2} = 4\sqrt{C} \frac{u_1}{u_\infty} \frac{T_1}{T_\infty} \frac{\left(1 - \frac{a_2}{5}\right)}{\sqrt{\lambda}} R_\infty^{-1/2} \quad (23)$$

The physical boundary-layer thickness in the xy -plane can be determined from transformation (10), and an explicit expression for it in terms of λ is given in appendix A.

The velocity profiles in the xt -plane are given by equation (16). These can be converted to the physical xy -plane by means of transformation (10). An explicit expression for y in terms of t is given in appendix A. The temperature profiles follow from the velocity profiles by means of equation (6a). It should be noted, however, that for most practical purposes it is not actually necessary to determine the profiles in the xy -plane. Skin friction (cf. equation (23)) and separation point,

¹It is demonstrated subsequently that the flow near a stagnation point is better represented by a fourth-degree velocity profile than by a sixth-degree profile. In such a region the expression for the skin-friction coefficient is altered in that the term $\left(1 - \frac{a_2}{5}\right)$ is replaced

by $\left(1 - \frac{a_2}{6}\right)$.

for example, can be determined directly from results in the xt -plane, while stability calculations (cf. appendix C) can be performed without use of the profiles in the xy -plane.

The equations developed thus far should be adequate for the practical determination of boundary-layer characteristics in most cases. There are, however, two important exceptions. These are: (a) The location of the separation point in an adverse pressure gradient and (b) the flow in the vicinity of a forward stagnation point. Item (a) is treated in the immediately succeeding paragraph, while item (b) is investigated in a later separate section.

Determination of Separation Point

Although the equations thus far developed will usually be found to lead to sufficiently accurate results for most boundary-layer characteristics even in flows with adverse pressure gradients, it will be found that the location of separation points will still be predicted with appreciable error. This error can be greatly diminished by a simple modification of the preceding equations.

For the purpose of determining the separation point, velocity profiles can be chosen which, in addition to satisfying boundary conditions (15), satisfy a further boundary condition at the separation point. The additional boundary condition is obtained by differentiating equation (1) twice with respect to t , and by then taking values at the wall at the point where $\partial u/\partial t = 0$. In this manner, with the use of equation (6a), the condition

$$\left[\frac{\partial^4 (u/u_1)}{\partial \tau^4} \right]_{\tau=0} = 0 \quad (24)$$

is obtained.

Condition (24) is strictly valid only at the separation point (where $\partial u/\partial y = 0$). Nevertheless, by using this condition for the entire flow, it seems plausible that the location of the separation point in any given case could be predicted with improved accuracy, since the value of the dimensionless boundary-layer thickness λ may be expected to be thereby more accurately determined at the separation point. This has already been shown by an example for incompressible flow in reference 2 and will be further shown by examples (table I) for compressible flow in the present analysis.

A seventh-degree polynomial in τ satisfying conditions (15) and (24) can be chosen. By proceeding in the same manner as (previously) with the sixth-degree profiles, the following solution λ_S for $\lambda(\xi)$, analogous to equation (22), is obtained (a detailed derivation is given in appendix B):

$$\lambda_S = \frac{32.83}{G} \frac{\int_0^\xi \left(\frac{u_1}{u_\infty}\right)^{6.128} \left(\frac{T_1}{T_\infty}\right)^{0.9366} d\xi}{\left(\frac{u_1}{u_\infty}\right)^{7.128} \left(\frac{T_1}{T_\infty}\right)^{2.437}} \quad (25)$$

The value of $\gamma = 1.4$ has been used in equation (25). In case the region of adverse pressure gradient follows a region of favorable pressure gradient, and hence starts at some point behind the leading edge, then equation (25) should be modified to equation (B4) in appendix B. Separation will occur at the point where (see appendix B):

$$\lambda_S = \frac{7}{G} \left(-\frac{u_\infty}{u_1'}\right) \frac{\left[1 + \frac{\gamma - 1}{2} M_\infty^2 \left(1 - \frac{u_1^2}{u_\infty^2}\right)\right]^{\frac{3-2\gamma}{\gamma-1}}}{1 + \left(\frac{\gamma - 1}{2}\right) M_\infty^2} \quad (26)$$

The location of the separation point is thus determined at the value of ξ for which equations (25) (or (B4)) and (26) give the same value of λ_S . For any given adverse pressure gradient (negative $u_1'(\xi)$) and free-stream Mach number M_∞ , the function $\lambda_S(\xi)$ can be plotted against ξ in accordance with both equation (25) (or equation (B4)) and equation (26) in the (anticipated) vicinity of the separation point. The point of intersection of these two curves is then the separation point.² It should be emphasized that equation (25)

²This point will, according to equations (25) and (26), be independent of G ; hence one may put $G = 1$ for this purpose. This does not imply that the separation point will actually be unaffected by a shock wave at the leading edge, since the values of $u_1/u_\infty(\xi)$ and $u_1'/u_\infty(\xi)$ may still contain the effect of such a wave.

is to be used only for determination of separation point. For other purposes, such as determination of skin-friction distribution or of critical Reynolds number, equation (22) and its related equations are to be used, even for a region in an adverse pressure gradient, unless properties close to or at the separation point are sought.

An application of the general solutions developed here, as well as a check on the accuracy of results obtained from them, will now be given by means of examples based on two different types of flow outside of the boundary layer.

FLOW WITH LINEARLY DIMINISHING VELOCITY

The case

$$\frac{u_1}{u_\infty} = 1 - b\xi \quad (27a)$$

where b is a positive constant, is now considered. This represents the simplest type of adverse pressure gradient. By introducing the linear change of variables

$$\left. \begin{aligned} \xi_1 &= b\xi \\ \lambda_1 &= b\lambda \end{aligned} \right\} \quad (28)$$

equation (14) remains unchanged, except that ξ is replaced by ξ_1 and λ , by λ_1 . Moreover, u_1/u_∞ now becomes

$$\frac{u_1}{u_\infty} = 1 - \xi_1 \quad (27b)$$

Thus the constant b no longer appears in the equations. Consequently, in this case it is actually necessary to solve equation (14) only for $b = 1$, since for any other value of b it is necessary only to replace ξ

by ξ_1 and λ by λ_1 in the solution obtained for $b = 1$. The present example, therefore, will treat the case

$$\frac{u_1}{u_\infty} = 1 - \xi \quad (27c)$$

A constant average value \bar{a}_2 for a_2 can be chosen by noting that in this case a_2 will vary from 0 (at $\xi = 0$) to 5 (at the separation point, where, according to equation (16), $1 - (a_2/5) = 0$). Consequently the value $\bar{a}_2 = 2.5$ may be chosen. Moreover, the value $\bar{a}_2^2 = 12.5$ will be used here. With these values, the approximate solution (22) for the case represented by equation (27c) without a shock wave ($G = 1$) at the leading edge becomes:

$$\lambda = \frac{37.5 \int_{\eta}^1 \eta^{5.50} \left[1 + \frac{\gamma - 1}{2} M_\infty^2 (1 - \eta^2) \right]^{5/4} d\eta}{\eta^{6.50} \left[1 + \left(\frac{\gamma - 1}{2} \right) M_\infty^2 (1 - \eta^2) \right]^{2.75}} \quad (29a)$$

where $\eta = 1 - \xi$. For zero Mach number, that is, $M_\infty = 0$, equation (29a) reduces to:

$$\lambda = 5.76 \left[(1 - \xi)^{-6.50} - 1 \right] \quad (29b)$$

The skin friction follows from equations (23) and (20), while the velocity profiles can be obtained, as previously explained, by means of equations (16) and (A2) (appendix A). For $M_\infty = 1$ and 3, the integration in equation (29a) was performed by expanding the integrand in a series according to the binomial theorem. The results for $\lambda(\xi)$, skin friction at the wall, and velocity profiles are shown in figures 1, 2, and 3, respectively, with $M_\infty = 0, 1, \text{ and } 3$.

The critical Reynolds number for the stability of the laminar boundary layer in the presence of small disturbances was calculated here on the basis of criteria developed by Lin and Lees (references 11 and 12). The method of calculation is outlined in appendix C, and the results for the critical Reynolds number $\rho_{\infty} u_{\infty} L / \mu_{\infty}$ at the station $\xi = 0.0496$ are given in table II for $M_{\infty} = 0, 1,$ and 3 . By comparing the results for zero Mach number with those for the critical Reynolds number (1,500,000) at the same station for the flow over a flat plate based on the solutions of reference 8 (see also reference 1), it is seen that the adverse pressure gradient is here highly destabilizing. Moreover, it can also be seen from table II that higher Mach numbers greatly destabilize the flow over an adiabatic wall.

As a check on the accuracy of approximate solution (22) to differential equation (14), equation (14) was solved exactly for this case for $M_{\infty} = 0$ and numerically by Adam's parabolic method (reference 13) with increments of $\Delta\xi = 0.01$ for $M_{\infty} \neq 0$. The solutions thus obtained for $\lambda(\xi)$ and for the profiles are shown in figures 1 and 3, respectively. The agreement between these solutions and those based on equation (22) is seen from these figures to be satisfactory for practical purposes. As a further check, the critical Reynolds number at $\xi = 0.0496$ was calculated for $M_{\infty} = 0$ by using the exact solution of equation (14). Table II indicates satisfactory agreement between this result $((R_{\infty})_c = 380,000)$ and that $((R_{\infty})_c = 330,000)$ based on equation (22).

It is thus indicated that equation (22) is a satisfactory approximation to an exact solution of differential equation (14). It is also desirable to check whether an exact solution of equation (14), or approximation (22), is a satisfactory approximation to an exact solution of the original partial differential equation (1). This would constitute a check on the practical reliability of the basic method used here, namely the extension of the Kármán-Pohlhausen method to sixth-degree profiles. Such a check can be made by comparing the results obtained by means of equations (14) and (22) with the results of Howarth (reference 4) for zero Mach number, based on an accurate solution of the original partial differential equations (1) and (3). Such a comparison is shown in figures 2 and 3 for skin friction and velocity profiles, respectively, and in table II for critical Reynolds number. In all cases the comparison indicates that the solutions obtained by means of the equations developed here give sufficiently reliable results for practical purposes.

The separation point is determined by equating the right sides of equations (25) and (26). In the present case the point at which these right sides are equal was determined by plotting $\lambda_S(\xi)$ according to

both equations (25) and (26) on the same sheet in the vicinity of $\xi = 0.14$ for $M_\infty = 0$ and 1 and $\xi = 0.10$ for $M_\infty = 3$. These are the vicinities in which, according to figure 1 (based on sixth-degree, not seventh-degree, profiles), separation might be expected to occur. The separation points determined by this means for $M_\infty = 0, 1,$ and 3 are shown in table I, together with the results of Stewartson (reference 5). The agreement between these two sets of results is seen to be exceptionally good.

For purposes of comparison, the separation point was also determined by the use of equation (22) and by means of the classical Kármán-Pohlhausen method based on fourth-degree profiles, the latter for zero Mach number only. The results are shown in table I. Although the use of the sixth-degree profiles (equation (22)) gives a more accurate location of the separation point than the fourth-degree profiles, the special use of the seventh degree (equations (25) and (26)) for this purpose gives here virtually the exact values.

It may be asked whether the seventh-, instead of the sixth-degree velocity profile could be used for determining the other boundary-layer characteristics, in addition to the separation point. Consequently, the skin friction and velocity profiles for the present case were determined on the basis of the seventh-degree velocity profile, in conjunction with equation (14) (cf. appendix B). It was found that the results, even at a station fairly close to the separation point, did not agree so closely with Howarth's solution (reference 4) as those based on the sixth-degree profile. It is therefore concluded that the seventh-degree profile should be used only as a means of determining the separation point in regions of adverse pressure gradients and that otherwise (except for flow near a stagnation point) the equations developed on the basis of the sixth-degree velocity profile should be used.

FLOW NEAR A FORWARD STAGNATION POINT

The case

$$\frac{u_1}{u_\infty} = b\xi \quad (30a)$$

represents physically the flow in the vicinity of a forward stagnation point, such as over the leading edge of a blunt object in subsonic flow.

As in the preceding case (equation (27a)) the constant b here can be eliminated by means of transformations (28). Hence only the case

$$\frac{u_1}{u_\infty} = \xi \quad (30b)$$

need be treated.

For zero Mach number ($M_\infty = 0$) an exact solution of ordinary differential equation (14) in the case represented by equation (30b) is of the form $\lambda = \text{Constant}$. This can also be seen from solution (22) for this case, with $\bar{a}_2 = a_2$ and $\overline{a_2^2} = a_2^2$, where according to equation (20) (with $M_\infty = 0$, $G = 1$, and $u_1'/u_\infty = 1$) $a_2 = -\lambda/2$. From equation (22), in fact, the following cubic in λ is obtained:

$$f(\lambda) = \lambda^3 + 37.43\lambda^2 - 979.4\lambda + 6435 = 0 \quad (31)$$

By plotting $f(\lambda)$ against λ , it is found that there are no physically significant roots of equation (31). Such a result was already obtained by Schlichting and Ulrich (reference 6). It will be found, however, that the curve $f(\lambda)$ against λ in the physically significant region comes relatively close to the λ -axis at a point when the curve has a local maximum value. If the value of λ at this point is taken for purposes of an approximation, then

$$\lambda = 9.481 \quad (32)$$

Since the approximation (32) does not appear to be satisfying in principle, the use of fourth-degree velocity profiles will be investigated for this case. The fourth-degree polynomial satisfying all the boundary conditions in equations (15) with the exception of the two conditions involving the third derivative of velocity ($\partial^3(u/u_1)/\partial\tau^3 = 0$ at $\tau = 0$ and at $\tau = 1$) is

$$\frac{u}{u_1} = \left(2 - \frac{a_2}{3}\right) + a_2\tau^2 - (2 + a_2)\tau^3 + \left(1 + \frac{a_2}{3}\right)\tau^4 \quad (33)$$

With the profile (33), equation (14) remains valid, but the F 's as defined by equations (12) are now given explicitly by the following expressions:

$$\left. \begin{aligned} F_1 &= 0.1175 + 0.00212a_2 - 0.000441a_2^2 \\ F_2 &= -0.3000 - 0.01667a_2 - \frac{\gamma - 1}{2} M_1^2 (0.4175 + \\ &\quad 0.01878a_2 - 0.000441a_2^2) \\ F_3 &= 2 - 0.3333a_2 \end{aligned} \right\} \quad (34)$$

Expressions (34) replace, in this case, expressions (18) based on sixth-degree profiles. For the case (30b) with $M_\infty = 0$, equation (14) leads to a cubic in λ whose physically significant root is now found to be (cf. also reference 3)

$$\lambda = 7.052 \quad (35)$$

To compare the accuracy of solution (32), based on sixth-degree velocity profiles, with that of solution (35), the skin friction, velocity profiles, and critical Reynolds number for laminar-flow stability have been calculated on the basis of both of the solutions. The results thus obtained, together with a comparison with results of an exact solution (reference 14) for this case, are shown in tables III and IV and in figure 4. From these comparisons it is seen that the solution based on fourth-degree profiles leads in this case to more accurate results than that based on sixth-degree profiles for the boundary-layer characteristics considered, including the critical Reynolds number. It may therefore be concluded that for a stagnation-flow case represented by equations (30a) and (30b), a satisfactory solution for practical purposes can be obtained by means of equations (33), (34), and (35) based on fourth-degree velocity profiles.

For $M_\infty \neq 0$, an approximate solution of equation (14) quite similar to equation (22) can be obtained for the present case. Using expressions (34) and putting $u_1/u_\infty = \xi$ in accordance with equation (30b), the following approximate solution is thus obtained:

$$\lambda = \frac{\frac{4}{F_1 G} \int_0^\xi \left[3 + \frac{2}{F_1} (0.1333 + 0.01667 \bar{a}_2) \left(\frac{T_1}{T_\infty} \right)^{\frac{\gamma}{\gamma-1}} - \frac{1}{F_1} (0.2508 + 0.01878 \bar{a}_2 - 0.000441 \bar{a}_2^2) \right] d\xi}{4 + \frac{2}{F_1} (0.1333 + 0.01667 \bar{a}_2) \left(\frac{T_1}{T_\infty} \right)^{\frac{2}{\gamma-1}} - \frac{1}{F_1} (0.2508 + 0.01878 \bar{a}_2 - 0.000441 \bar{a}_2^2)} \quad (36)$$

where F_1 is now given by equation (34). At the leading edge ($\xi = 0$) the value λ_0 of λ will be, according to equation (36),

$$\lambda_0 = \frac{2}{G} \frac{\left(1 + \frac{\gamma-1}{2} M_\infty^2 \right)^{\frac{\gamma-2}{\gamma-1}}}{\left(0.1333 + 0.01667 \bar{a}_2 + 2F_1 \right)} \quad (36a)$$

As a numerical example, the case $M_\infty = 1$ was calculated by means of equations (36) and (36a), assuming $\bar{a}_2 = -4.48$ and $\bar{a}_2^2 = 20.1$. The results for $\lambda(\xi)$, skin friction, and velocity profiles are shown in figures 5, 6, and 7, together with the results for $M_\infty = 0$.

CONCLUSIONS

From the foregoing analysis, based on an extension of the Kármán-Pohlhausen method primarily to sixth-degree velocity profiles for determining laminar-boundary-layer characteristics in the compressible flow over an adiabatic wall in the presence of an axial pressure gradient, the following main conclusions can be drawn.

1. For a given free-stream Mach number and a given velocity distribution outside of the boundary layer, a relatively simple general approximate solution to the boundary-layer equations has been derived for a Prandtl number of unity and for a linear relation between the viscosity coefficient and the temperature. This solution not only is convenient

to apply but also leads to results which will be sufficiently accurate for most practical purposes, including determination of critical Reynolds number.

2. For the particular purpose of determining the location of the separation point in a region of adverse pressure gradient, a relatively quick and simple method has been given here, based on the use of seventh-degree velocity profiles. The numerical example indicated that the results thus obtained should in general be quite accurate.

3. In the special case of flow near a forward stagnation point, the Kármán-Pohlhausen method with fourth-degree velocity profiles gives results of very satisfactory accuracy, even for the critical Reynolds number.

4. The numerical examples given here illustrate the destabilizing influences of an adverse pressure gradient and of a Mach number greater than zero.

Polytechnic Institute of Brooklyn
Brooklyn, N. Y., May 28, 1951

APPENDIX A

PHYSICAL BOUNDARY-LAYER THICKNESS

Results in the xt -plane can be transformed into the physical xy -plane by means of relation (10). Thus

$$y/\delta_t = \int_0^\tau (T/T_1) d\tau \quad (A1)$$

By inserting velocity profile (16) and equations (19a) and (19b) into expression (6a) for (T/T_1) , equation (A1) yields:

$$\begin{aligned} \frac{y}{\delta_t} = & \tau - \frac{\gamma - 1}{2} M_\infty^2 \frac{(u_1/u_\infty)^2}{1 + \frac{\gamma - 1}{2} M_\infty^2 \left(1 - \frac{u_1^2}{u_\infty^2}\right)} \left\{ -\tau + \frac{4}{3} \left(1 - \frac{a_2}{5}\right)^2 \tau^3 + \right. \\ & a_2 \left(1 - \frac{a_2}{5}\right) \tau^4 + \frac{a_2^2}{5} \tau^5 - \frac{2}{3} (5 + 2a_2) \left(1 - \frac{a_2}{5}\right) \tau^6 + \\ & \left[\frac{8}{7} (3 + a_2) \left(1 - \frac{a_2}{5}\right) - \frac{2}{7} a_2 (5 + 2a_2) \right] \tau^7 + \\ & \left[\frac{a_2}{2} (3 + a_2) - \frac{1}{2} \left(1 - \frac{a_2}{5}\right) \left(2 + \frac{3}{5} a_2\right) \right] \tau^8 + \\ & \frac{1}{9} \left[(5 + 2a_2)^2 - 2a_2 \left(2 + \frac{3}{5} a_2\right) \right] \tau^9 - \\ & \frac{2}{5} (3 + a_2) (5 + 2a_2) \tau^{10} + \\ & \left[\frac{2}{11} (5 + 2a_2) \left(2 + \frac{3}{5} a_2\right) + \frac{4}{11} (3 + a_2)^2 \right] \tau^{11} - \\ & \left. \frac{1}{3} (3 + a_2) \left(2 + \frac{3}{5} a_2\right) \tau^{12} + \frac{1}{13} \left(2 + \frac{3}{5} a_2\right)^2 \tau^{13} \right\} \quad (A2) \end{aligned}$$

After $\delta_t(\xi)$ has been obtained, the point ξ, y in the physical plane corresponding to any given point ξ, τ in the mathematical plane can be directly determined by means of equation (A2).

The boundary-layer thickness δ in the physical plane is the value of y at which $\tau = 1$. Hence, by putting $\tau = 1$ in equation (A2), the following explicit expression is obtained for the boundary-layer thickness:

$$\frac{\delta}{\delta_t} = 1 + \frac{\frac{(\gamma - 1)}{2} M_\infty^2 \left(\frac{u_1}{u_\infty}\right)^2}{1 + \frac{\gamma - 1}{2} M_\infty^2 \left(1 - \frac{u_1^2}{u_\infty^2}\right)} \left(0.3950 + 0.02116a_2 - 0.000622a_2^2\right) \quad (A3)$$

APPENDIX B

DETERMINATION OF SEPARATION POINT

A seventh-degree-polynomial velocity profile satisfying condition (24) in addition to conditions (15) is

$$\frac{u}{u_1} = \left(\frac{7}{4} - \frac{a_2}{2}\right)\tau + a_2\tau^2 - \frac{1}{4}(21 + 10a_2)\tau^5 + (7 + 3a_2)\tau^6 - \left(\frac{5}{2} + a_2\right)\tau^7 \quad (B1)$$

where a_2 is given by equation (20). With the profile (B1), the F 's as defined by equations (12) become (a subscript s is used for the present results to distinguish them from the corresponding results based on sixth-degree profiles):

$$\left. \begin{aligned} F_{1s} &= 0.1156 + 0.00253a_2 - 0.001454a_2^2 \\ F_{2s} &= -0.02976a_2 - 0.3125 - \frac{\gamma - 1}{2} M_1^2 (0.4281 + \\ &\quad 0.03229a_2 - 0.00145a_2^2) \\ F_{3s} &= 1.7500 - 0.5000a_2 \end{aligned} \right\} \quad (B2)$$

The separation point will be located where $\left[\frac{\partial(u/u_1)}{\partial\tau}\right]_0 = 0$; it therefore follows from equation (B1) that laminar-flow separation will occur at the point where $a_2 = 3.5$. By using expressions (B2) and assuming, as in the section entitled "General Approximate Solutions,"

that in the expressions for F_{1s} and F_{2s} the quantities a_2 and a_2^2 may, as an approximation, be replaced by constant values \bar{a}_2 and \bar{a}_2^2 , the following approximate solution λ_s for $\lambda(\xi)$ of differential equation (14) (with F_1 , F_2 , and F_3 replaced by F_{1s} , F_{2s} , and F_{3s} , respectively) is obtained:

$$\lambda_s = \frac{\frac{7}{2} \frac{1}{F_{1s} G} \int_0^\xi \left(\frac{u_1}{u_\infty}\right)^{3 + \frac{2}{F_{1s}}(0.0625 + 0.02976\bar{a}_2)} \left(\frac{T_1}{T_\infty}\right)^{\frac{\gamma}{\gamma-1} - \frac{1}{F_{1s}}(0.1781 + 0.03229\bar{a}_2 - 0.00145\bar{a}_2^2)} d\xi}{\left(\frac{u_1}{u_\infty}\right)^4 + \frac{2}{F_{1s}}(0.0625 + 0.02976\bar{a}_2) \left(\frac{T_1}{T_\infty}\right)^{\frac{2}{\gamma-1} - \frac{1}{F_{1s}}(0.1781 + 0.03229\bar{a}_2 - 0.00145\bar{a}_2^2)}} \quad (B3)$$

Since the main object of equation (B3) is to determine the separation point, the values of \bar{a}_2 and \bar{a}_2^2 may for this purpose be chosen as those which a_2 and a_2^2 would actually have at that point. Hence, for determining the separation point, the values $\bar{a}_2 = 3.5$ and $\bar{a}_2^2 = 12.25$ are inserted into equation (B3). With $\gamma = 1.4$, expression (25) for $\lambda_s(\xi)$ then results.

Since separation occurs where $a_2 = 3.5$ and since a_2 , which is proportional to λ , is given by equation (20), the value of λ at which separation occurs will be that given by equation (26) in the main text.

Equations (B3) and (25) for $\lambda_s(\xi)$ are valid only under the boundary condition $\lambda_s = 0$ at $\xi = 0$. In case the region of adverse pressure gradient starts at some point $\xi = \xi_a$ other than the leading edge, this boundary condition must be replaced by the condition $\lambda_s = \lambda_a$ at $\xi = \xi_a$. Solution (25) for $\lambda_s(\xi)$ must then be replaced by the following solution (with $\bar{a}_2 = 3.5$ and $\bar{a}_2^2 = 12.25$):

$$\lambda_s = \frac{\frac{32.83}{G} \int_{\xi_a}^\xi \left(\frac{u_1}{u_\infty}\right)^{6.128} \left(\frac{T_1}{T_\infty}\right)^{0.9366} d\xi + \lambda_a \left[\left(\frac{u_1}{u_\infty}\right)^{7.128} \left(\frac{T_1}{T_\infty}\right)^{2.437} \right]_{\xi=\xi_a}}{\left(\frac{u_1}{u_\infty}\right)^{7.128} \left(\frac{T_1}{T_\infty}\right)^{2.437}} \quad (B4)$$

The value of λ_a is obtained directly from equation (22) of the main text. Thus

$$\lambda_a = \frac{4}{F_1 G} \frac{\int_0^{\xi_a} \left(\frac{u_1}{u_\infty}\right)^{3 + \frac{2}{F_1}(0.08571 + 0.01905\bar{a}_2)} \left(\frac{T_1}{T_\infty}\right)^{\frac{\gamma}{\gamma-1} - \frac{1}{F_1}(0.1950 + 0.02116\bar{a}_2 - 0.000622\bar{a}_2^2)} d\xi}{\left(\frac{u_1}{u_\infty}\right)^{4 + \frac{2}{F_1}(0.08571 + 0.01905\bar{a}_2)} \left(\frac{T_1}{T_\infty}\right)^{\frac{2}{\gamma-1} - \frac{1}{F_1}(0.1950 + 0.02116\bar{a}_2 - 0.000622\bar{a}_2^2)} \Big|_{\xi=\xi_a}} \quad (B5)$$

APPENDIX C

DETERMINATION OF CRITICAL REYNOLDS NUMBER

In accordance with the procedure outlined by Lees in reference 11, the critical Reynolds number at a given station x for the stability of the laminar boundary layer can be determined in the following manner. It is required first to determine the value of y/l such that

$$(1 - 2\beta) \left(\frac{\alpha}{0.580} \right) - 1 = 0 \quad (C1)$$

where

$$\alpha = - \frac{\pi \left[\left(\frac{u}{u_1} \right)' \right]_0 \left(\frac{u}{u_1} \right) \frac{T}{T_1} \left[\left(\frac{u}{u_1} \right)'' - \frac{\left(\frac{T}{T_1} \right)'}{\left(\frac{u}{u_1} \right)'} \right]}{\left[\left(\frac{u}{u_1} \right)' \right]_0^2 \frac{T_0}{T_1} \left[\left(\frac{u}{u_1} \right)' - \frac{\left(T \right)'}{\left(\frac{u}{u_1} \right)'} \right]} \quad (C2)$$

$$\beta = \frac{\left[\left(\frac{u}{u_1} \right)' \right]_0 \frac{y}{l}}{\left(\frac{u}{u_1} \right)} - 1$$

the prime here denotes differentiation with respect to y/l and l is a convenient length. In the present analysis the quantity δ_t was chosen for l , except in the case of Howarth's series solution (reference 4) of the partial differential equations, where the quantity $2(vx/u_\infty)^{1/2}$ was chosen for l .

The appropriate value of y/l satisfying equation (C1) must usually be found graphically by trial. After this value has been determined, the critical Reynolds number based on l and on local values can be obtained from the expression:

$$(R_l)_c \equiv \left(\frac{u_1 l}{v_1}\right)_c = \frac{250 \left(\frac{T}{T_1}\right)_c^2 \left[\left(\frac{u}{u_1}\right)'\right]_o}{\left(\frac{u}{u_1}\right)_c^4 \left[1 - M_1^2 \left(1 - \frac{u}{u_1}\right)_c^2\right]^{1/2}} \quad (C3)$$

where the subscript c denotes values at the point where equation (C1) is satisfied.

For compressible flow it is more convenient to perform calculations in the xt-plane than in the xy-plane. With $l = \delta_t$, the foregoing relations can be expressed directly in the xt-plane by use of the relations:

$$\frac{\partial}{\partial(y/l)} = \frac{\partial \tau}{\partial(y/l)} \left(\frac{\partial}{\partial \tau}\right) = \frac{T_1}{T} \frac{\partial}{\partial \tau}$$

$$\frac{\partial^2}{\partial(y/l)^2} = \left(\frac{T_1}{T}\right)^2 \frac{\partial^2}{\partial \tau^2} + \frac{T_1}{T} \frac{\partial(T_1/T)}{\partial \tau} \left(\frac{\partial}{\partial \tau}\right)$$

where $\tau = t/\delta_t$. Using a dot (·) to denote differentiation with respect to τ , equations (C2) and (C3) become

$$\alpha = -\pi \frac{\left(\frac{T}{T_o}\right) \left[\left(\frac{u}{u_1}\right)'\right]_o \left(\frac{u}{u_1}\right) \left[\frac{\left(\frac{u}{u_1}\right)''}{\left(\frac{T_1}{T}\right) \left(\frac{u}{u_1}\right)'} - 2 \left(\frac{T}{T_1}\right)' \right]}{\left(\frac{T_o}{T_1}\right) \left[\left(\frac{u}{u_1}\right)'\right]^2} \quad (C4)$$

$$\beta = \frac{\left(\frac{T_1}{T_o}\right) \left[\left(\frac{u}{u_1}\right)'\right]_o \left(\frac{y}{\delta_t}\right)}{\left(\frac{u}{u_1}\right)} - 1$$

$$(R\delta_t)_c \equiv \left(\frac{u_1\delta_t}{v_1}\right)_c = \frac{25C\left(\frac{T}{T_1}\right)_c^2 \frac{T_1}{T_0} \left[\left(\frac{u}{u_1}\right)_c\right]_0}{\left(\frac{u}{u_1}\right)_c^4 \left[1 - M_1^2 \left(1 - \frac{u}{u_1}\right)_c^2\right]^{1/2}} \quad (C5)$$

The quantity y/δ_t in terms of τ is given by equation (A2) in appendix A; the trial value of τ (instead of y/l) must now be found which satisfies equation (C1).

REFERENCES

1. Libby, P. A., Morduchow, M., and Bloom, M.: A Critical Study of Integral Methods in Compressible Laminar Boundary Layers. NACA TN 2655, 1952.
2. Timman, R.: A One Parameter Method for the Calculation of Laminar Boundary Layers. Rep. F. 35, Nationaal Luchtvaartlaboratorium, 1949.
3. Dryden, Hugh L.: Computation of the Two-Dimensional Flow in a Laminar Boundary Layer. NACA Rep. 497, 1934.
4. Howarth, L.: On the Solution of the Laminar Boundary Layer Equations. Proc. Roy. Soc. (London), ser. A, vol. 164, no. 919, Feb. 18, 1938, pp. 547-579.
5. Stewartson, K.: Correlated Incompressible and Compressible Boundary Layers. Proc. Roy. Soc. (London), ser. A, vol. 200, no. 1060, Dec. 22, 1949. pp. 84-100.
6. Schlichting, H., and Ulrich, A.: Zur Berechnung des Umschlages laminar turbulent. Jahrb. 1942 deutschen Luftfahrtforschung, pt. I, R. Oldenburg (Munich), pp. 8-36.
7. Chapman, Dean R.: Laminar Mixing of a Compressible Fluid. NACA Rep. 958, 1950. (Supersedes NACA TN 1800.)
8. Chapman, D. R., and Rubesin, M. W.: Temperature and Velocity Profiles in the Compressible Laminar Boundary Layer with Arbitrary Distribution of Surface Temperature. Jour. Aero. Sci., vol. 16, no. 9, Sept. 1949, pp. 547-565.
9. Weil, Herschel: Effects of Pressure Gradient on Stability and Skin Friction in Laminar Boundary Layers in Compressible Fluids. Jour. Aero. Sci., vol. 18, no. 5, May 1951, pp. 311-318.
10. Scarborough, James B.: Numerical Mathematical Analysis. Second ed., The Johns Hopkins Press (Baltimore), 1950.
11. Lin, Chia Chiao, and Lees, Lester: Investigation of the Stability of the Laminar Boundary Layer in a Compressible Fluid. NACA TN 1115, 1946.
12. Lees, Lester: The Stability of the Laminar Boundary Layer in a Compressible Fluid. NACA Rep. 876, 1947.

13. V. Kármán, Theodore, and Biot, Maurice A.: *Mathematical Methods in Engineering*. McGraw-Hill Book Co., Inc., 1940.
14. Falkner, V. M., and Skan, Sylvia W.: *Some Approximate Solutions of the Boundary Layer Equations*. R. & M. No. 1314, British A.R.C., 1930.

TABLE I

SEPARATION POINTS CALCULATED BY APPROXIMATE METHOD (EQUATIONS (25) AND (26))

COMPARED WITH STEWARTSON'S SOLUTION AND WITH OTHER CALCULATIONS

$$\left[\frac{u_1}{u_\infty} = 1 - \xi \right]$$

| Method | ξ at separation point for M_∞ of - | | |
|--|---|-------|--------|
| | 0 | 1 | 3 |
| Method of equations (25) and (26) | 0.122 | 0.113 | 0.0768 |
| Stewartson's solution (reference 5) | .120 | .110 | .077 |
| Method based on sixth-degree profile (equation (22)) | .143 | .136 | .102 |
| Method based on fourth-degree profile | .156 | ----- | ----- |



TABLE II

VALUES OF CRITICAL REYNOLDS NUMBER FOR STABILITY AS CALCULATED

FROM APPROXIMATE SOLUTION (EQUATION (22)) OF EQUATION (14)

COMPARED WITH OTHER SOLUTIONS FOR ZERO MACH NUMBER

$$\left[\frac{u_1}{u_\infty} = 1 - \xi; \xi = 0.0496 \right]$$

| Method | $(R_\infty)_c$ for M_∞ of - | | |
|--|------------------------------------|---|---|
| | 0 | 1 | 3 |
| Approximate method, sixth-degree profile (equation (22)) | 330×10^3 | $\frac{120 \times 10^3 \left(1 + \frac{S}{T_\infty}\right)^3}{\left(1.2 + \frac{S}{T_\infty}\right) \left(1.01936 + \frac{S}{T_\infty}\right)^2}$ | $\frac{1600 \left(1 + \frac{S}{T_\infty}\right)^3}{\left(2.8 + \frac{S}{T_\infty}\right) \left(1.1742 + \frac{S}{T_\infty}\right)^2}$ |
| Exact solution of equation (14) | 380 | ----- | ----- |
| Howarth's series solution (reference 4) | 290 | ----- | ----- |
| Flat-plate flow (reference 8) | 1500 | ----- | ----- |

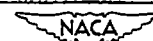


TABLE III

COMPARISON OF CALCULATED SKIN-FRICTION COEFFICIENTS

$$\left[\frac{u_1}{u_\infty} = \xi; M_\infty = 0 \right]$$

| Method | $R_\infty^{1/2} C_f / \xi$ |
|---|----------------------------|
| Fourth-degree profile (equation (35)) | 2.390 |
| Sixth-degree profile (equation (32)) | 2.530 |
| Solution of Falkner and Skan (reference 14) | 2.468 |



TABLE IV

COMPARISON OF CALCULATED CRITICAL REYNOLDS NUMBERS FOR STABILITY

$$\left[\frac{u_1}{u_\infty} = \xi; M_\infty = 0 \right]$$

| Method | $(R_\infty)_c \xi^2$ |
|---|----------------------|
| Fourth-degree profile (equation (35)) | 210×10^6 |
| Sixth-degree profile (equation (32)) | 170 |
| Solution of Falkner and Skan (reference 14) | 240 |



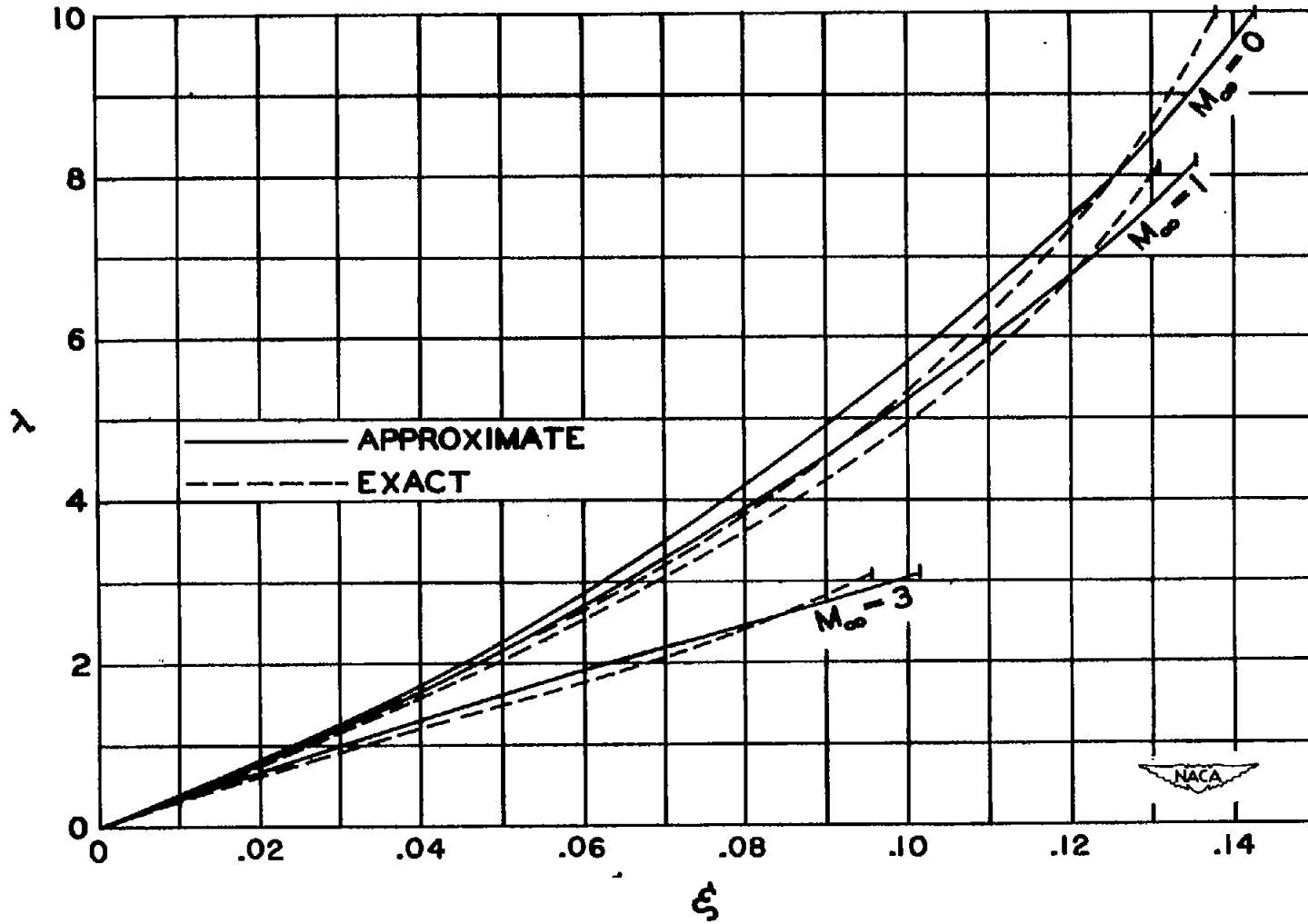


Figure 1.- Comparison between approximate solution (equation (22)) and exact solution of ordinary differential equation (equation (14)).
 Curves terminate at separation point. $u_1/u_\infty = 1 - \xi$.

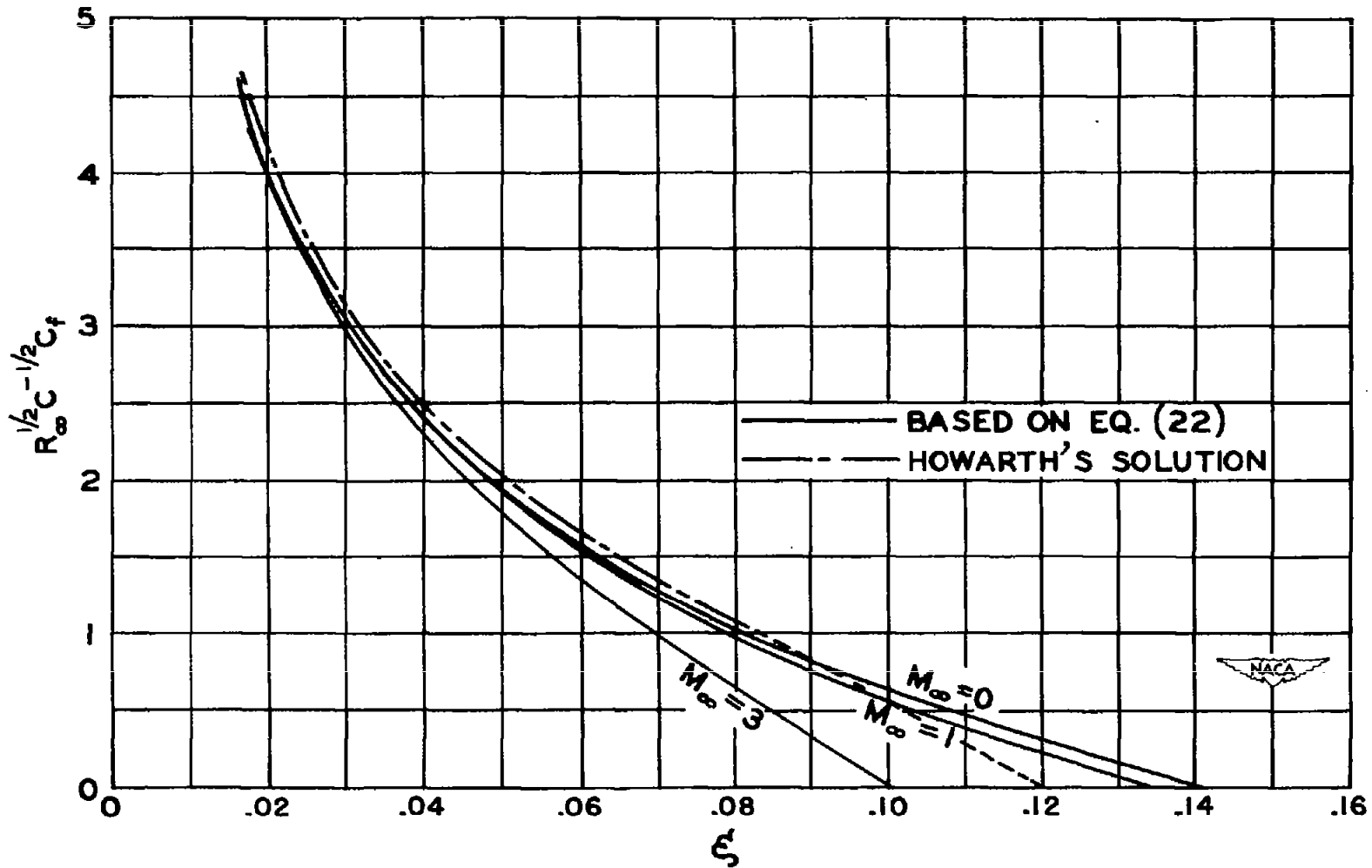


Figure 2.- Skin-friction coefficients obtained by approximate solution (equation (22)) of ordinary differential equation (equation (14)) compared with Howarth's solution for $M_\infty = 0$ (reference 4).
 $u_1/u_\infty = 1 - \xi$.

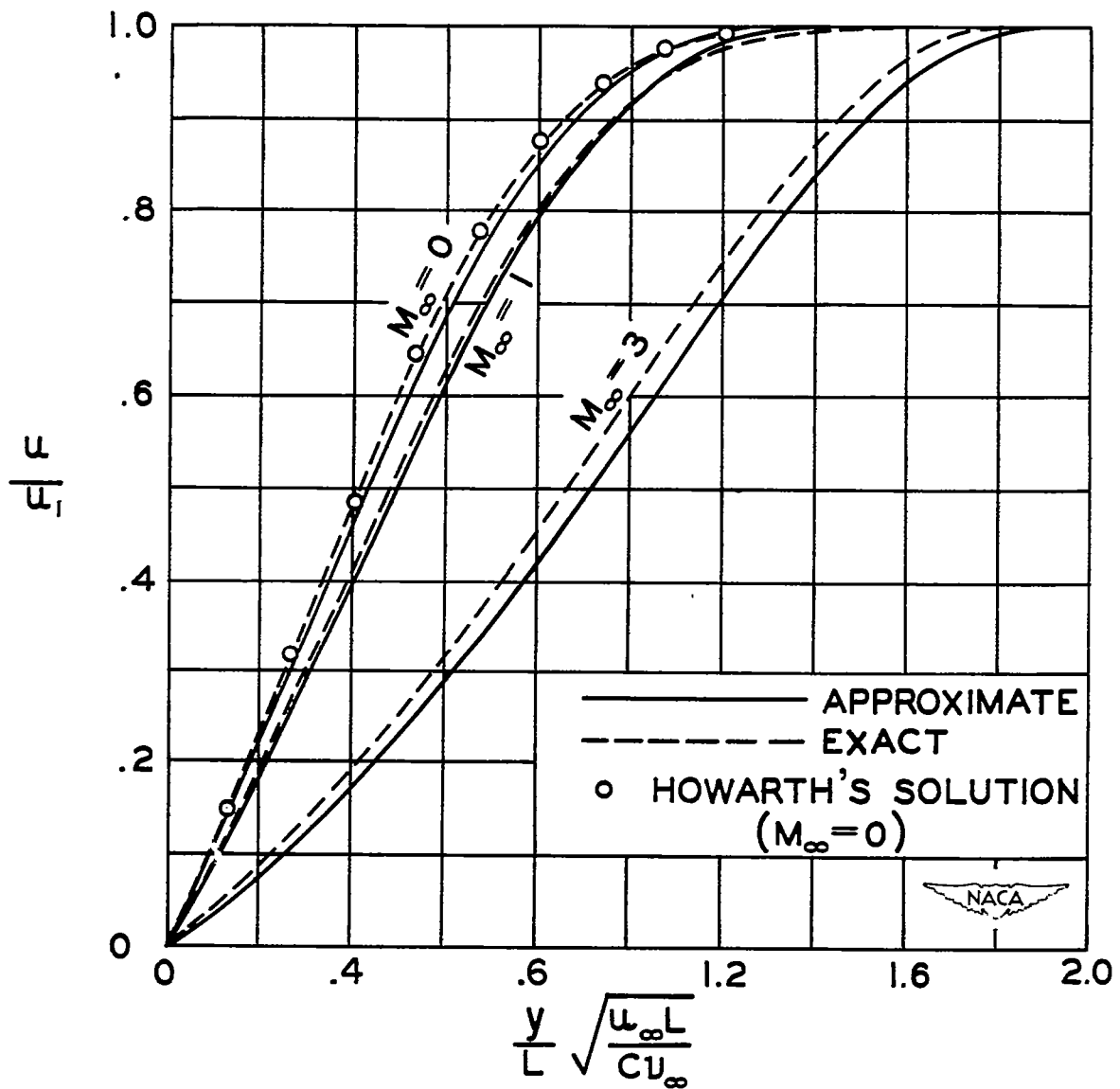


Figure 3.- Comparison of velocity profiles obtained from approximate solution (equation (22)) and exact solution of ordinary differential equation (equation (14)). $u_1/u_\infty = 1 - \xi$; $\xi = 0.0495$.

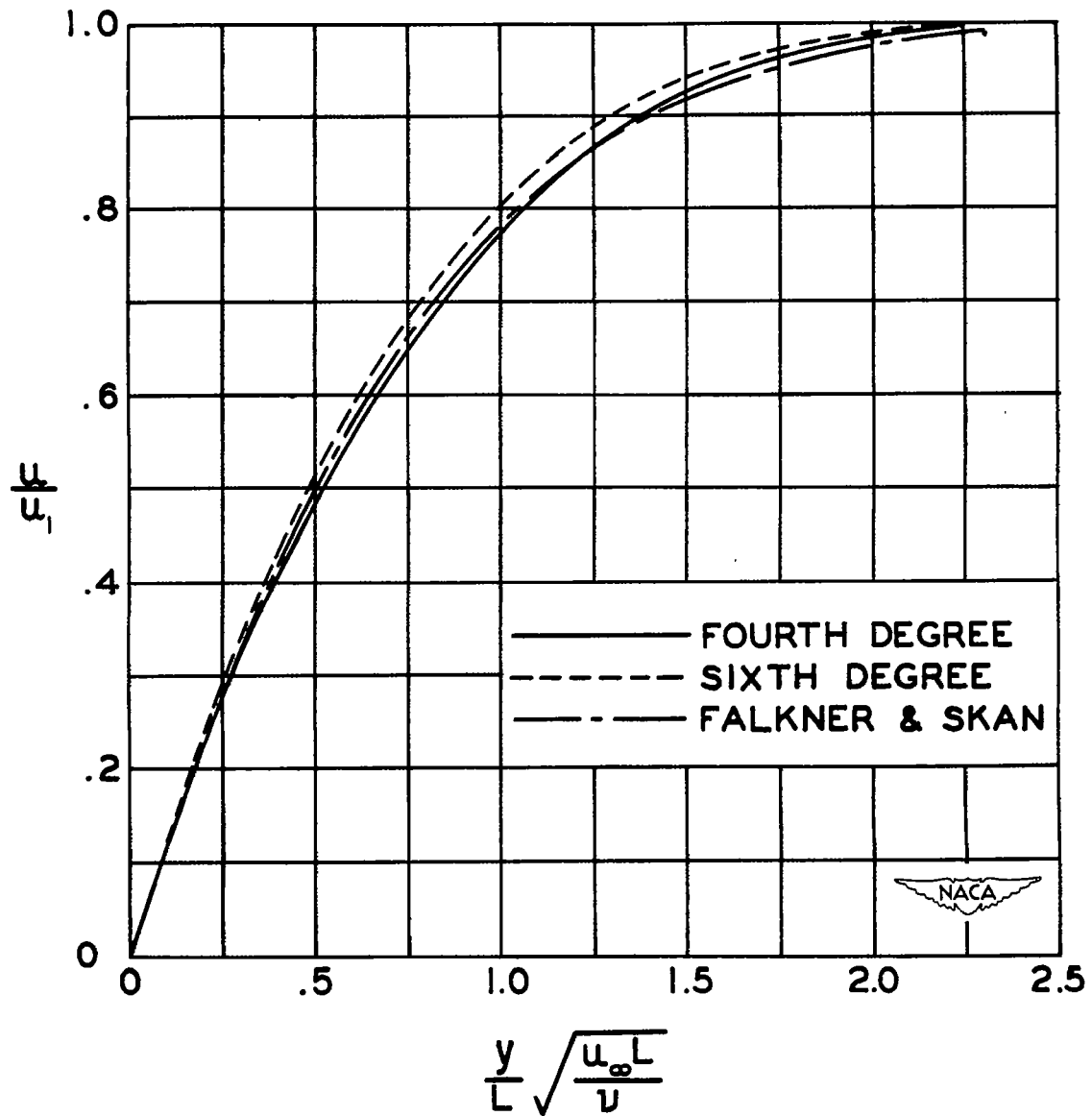


Figure 4.- Comparison of fourth- and sixth-degree velocity profiles with solution of Falkner and Skan (reference 14). $u_1/u_\infty = \xi$; $M_\infty = 0$.

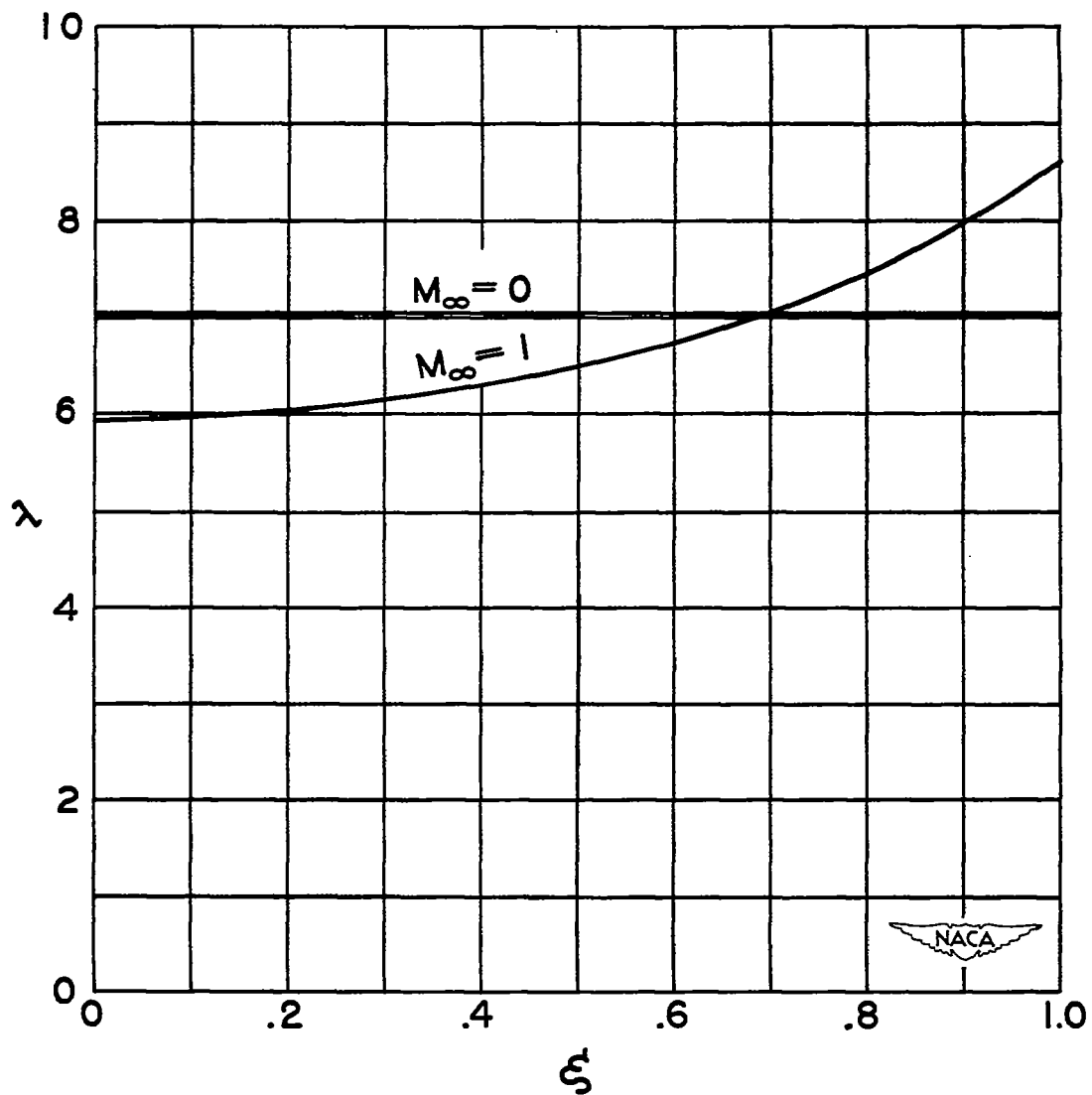


Figure 5.- Approximate solution (equation (36)) of ordinary differential equation (equation (14)); fourth-degree velocity profile. $u_1/u_\infty = \xi$.

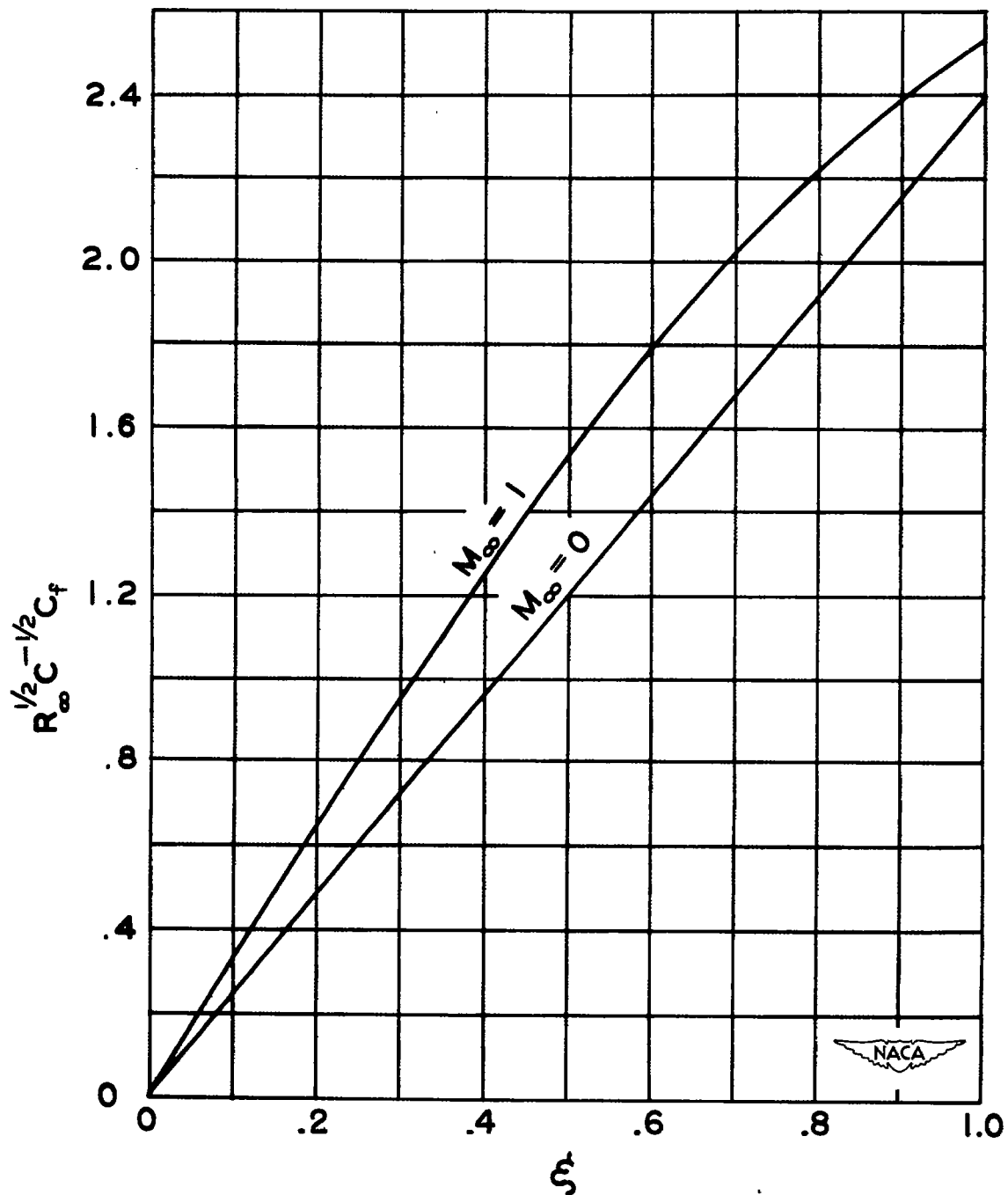


Figure 6.- Skin-friction coefficients based on approximate solution (equation (36)) of ordinary differential equation (equation (14)); fourth-degree velocity profile. $u_1/u_\infty = \xi$.

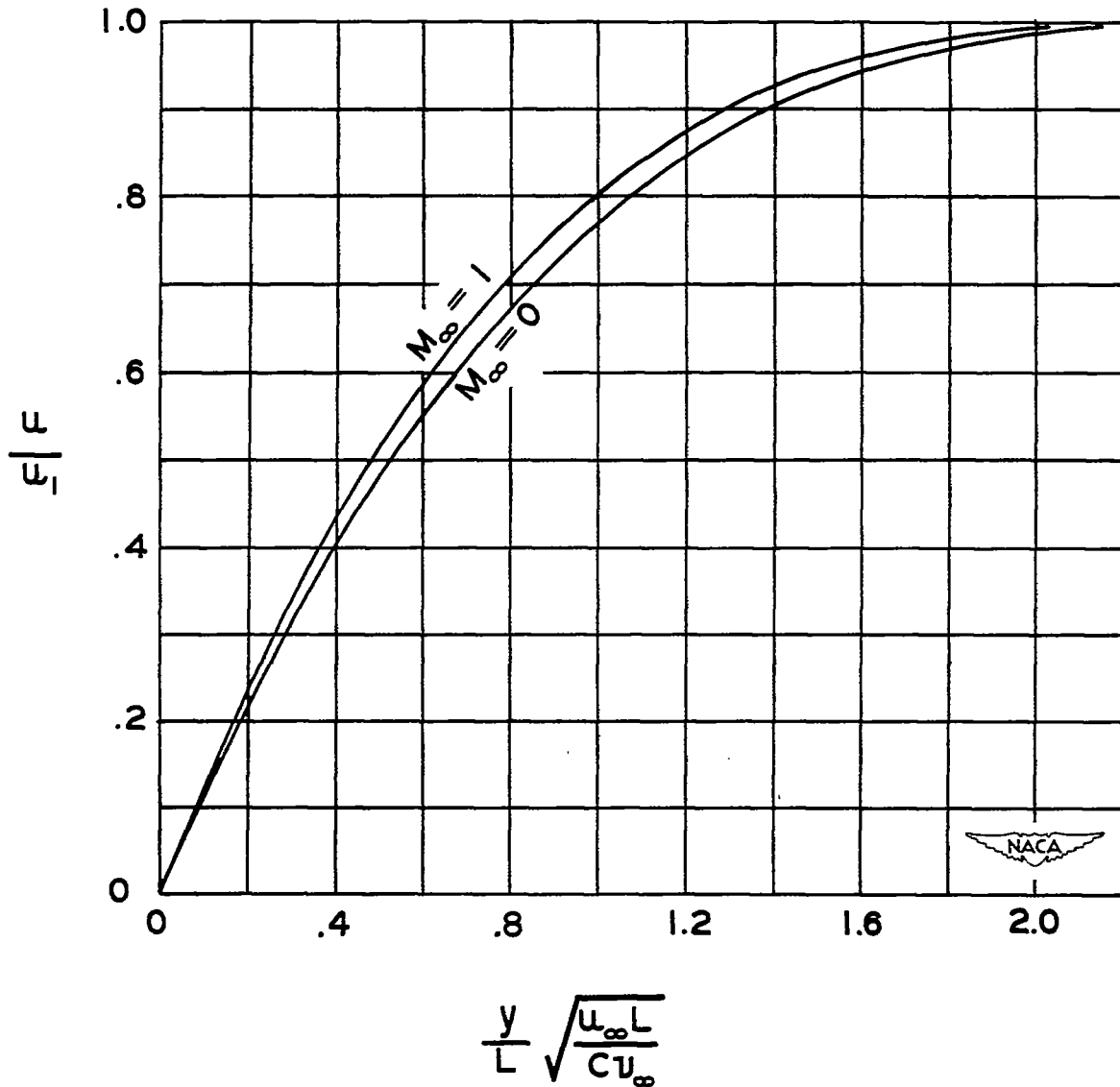


Figure 7.- Velocity profiles based on approximate solution (equation (36)) of ordinary differential equation (equation (14)); fourth-degree velocity profile. $u_1/u_\infty = \xi$; $\xi = 0.4$.